energies

MDPI

Article

Measurement of Static Frequency Characteristics of Home Appliances in Smart Grid Systems

Anton Beláň, Boris Cintula, Matej Cenký *, Peter Janiga, Jozef Bendík, Žaneta Eleschová and Adam Šimurka

Faculty of Electrical Engineering and Information Technology, Slovak University of Technology in Bratislava, Ilkovičova 3, 81 219 Bratislava, Slovakia; anton.belan@stuba.sk (A.B.); boris.cintula@stuba.sk (B.C.); peter.janiga@stuba.sk (P.J.); jozef.bendik@stuba.sk (J.B.); zaneta.eleschova@stuba.sk (Ž.E.); adam.simurka@stuba.sk (A.Š.)

* Correspondence: matej.cenky@stuba.sk; Tel.: +421-2-602-91-299

Abstract: The current transformation of power systems is aiming towards distributed source integration and general decentralization. Renewable energy sources and support of local energy supply create conditions for widespread use of new technologies and smart grids. As the electrical grids become more electrically independent, the importance of frequency control will rise. Stability of the system in such cases is no longer only relying on rotating inertia of generators as in the centralized grid. This known scenario has already been analyzed by many with computational models for optimal safety precautions of the grid. This paper aims to update the common home appliance frequency characteristics through measurements and compare them to those currently used. These devices were divided into two groups: general categorization and light sources. Subsequently, the frequency sensitivity coefficients were evaluated and analyzed home appliances were sorted into three categories according to the size of their frequency sensitivity coefficient values: positive, negative, and no effect. The results were compared with studies aimed at evaluating the static load characteristics. A simplified simulation of the frequency control, presented in the discussion section, was carried out to determine the consequences of the newly measured characteristics and concludes the paper.

Keywords: static load characteristics; frequency sensitivity coefficient; frequency response; home appliances measurement; smart grid

Citation: Beláň, A.; Cintula, B.; Cenký, M.; Janiga, P.; Bendík, J.; Eleschová, Ž.; Šimurka, A. Measurement of Static Frequency Characteristics of Home Appliances in Smart Grid Systems. *Energies* **2021**, *14*, 1739. https://doi.org/10.3390/en14061739

Academic Editor: Ashish Prakash Agalgaonkar

Received: 22 January 2021
Accepted: 17 March 2021
Published: 21 March 2021

1. Introduction

The power system is a complex nonlinear system in which operational safety and reliability are the highest priority; these are ensured by meeting the requirements of its stability. According to [1–4], the stability of such a system can be defined as its ability to regain a state of operating equilibrium after being subjected to a physical disturbance so that the entire system remains intact. The assessment of stability involves determining the nature of the influencing instability, the significance of the disturbance, as well as the time frame [1–4]. Earlier research studies in the field of frequency stability tended to focus primarily on generator behavior. Even though study of the load influence on the dynamic behavior of the system was also justified, this issue was investigated as a marginal problem. Today, it is evident that the quantification of load behavior in the system is an equally important factor in dynamic simulations [5]. On the other hand, load modeling is qualitatively different from generator modeling in many aspects [6]. These difficulties include the stochastic nature of the load, the number of load nodes in a power system, the lack of data surrounding the load, and also uncertainties regarding the characteristics of many load components (particularly for frequency variations) [5,7,8]. As for the most common example, after a sudden disturbance or fault, a temporary frequency in the system can lead to a substandard operation of devices. Furthermore, lower or higher temporal

frequencies deviating from the nominal value of 50 Hz (60 Hz) could cause malfunctions or even damage the connected equipment. Frequency control mechanisms were therefore developed to overcome these situations. To further reduce any possible risks, power system studies have to pursue better models for system components, including better load models [9]. This consideration has an even more topical dimension in the current state of power system transformation, which occurs due to the increase in decentralized energy resources and local energy supply support, which create conditions for widespread use of new technologies and smart grids.

The smart grid can be described as an electrical grid that can sensibly integrate the activities of all its users using digital technologies, enabling two-way communication between participants of the electricity market to improve distribution efficiency, energy use, and other energy measures. Technically, these factors create a precondition for perceiving the smart grid to a certain extent as a local small power system in an island operation. The concept of such a system can be formed by households, small businesses, and their combination with a high probability of penetration of the renewables. Consumption will then consist of a large number and different equipment/devices, depending on the type of customers. The downside may be that a large part of the power supply is dependent on weather conditions, therefore predetermining the possible power fluctuations with the ability to significantly affect the frequency in such a small network. Additionally, these factors combined with contingencies present an increased risk of power system operation and the equipment connected to the system.

The abovementioned reasons confirm the need to consider load characteristics in dynamic simulations, especially for small island plants with higher risk. Accurate load modeling signifies a vital role in analyzing the frequency stability of the power system [10,11]. Undoubtedly, the load characteristics should be included in the dynamic calculations due to more accurate results and minor frequency deviations. Our experimental measurement confirms different behavior of the observed home appliances when using different frequencies, providing their individual static frequency characteristics as a result. Subsequently, the impacts of these findings are demonstrated as a simplified model of frequency control. The main purpose of the article is justified by the results, and an additional discussion of possible further extension of these measurements is presented.

This article is organized as follows: Section 1 presents a current state-of-the-art situation and literature review; Section 2 introduces the measurement methodology and data analysis; Section 3 contains measurement results; Section 4 applies measured results into simplified simulation model of frequency control; Section 5 concludes the paper. Discussions about measurement and simulation results have separate subsections within their main sections as well.

Literature Review

One of the earliest thorough studies was conducted by Concordia and Ihara in 1982 [6], where much of the basic electrical equipment was studied and divided into categories, mostly considering the appearance of motors in the equipment. However, data collected in this article are possibly no longer accurate enough because of the nearly 30-year gap and very few other measurements being taken and published. In [5], the authors highlight the need for proper modeling considerations, including load dynamic characteristics. The requirement was based on the questionnaire sent to major industry representatives in North America, of which approximately 50% were unsatisfied with the currently used load models. Further improvement of load models has been divided into the measurements [12,13] and the mathematical model creation [13–19]. As the models are evolving and the electrical devices are changing, there is a necessity for updating such load characteristics for appliances. There are studies considering the detailed planning of the distribution networks based on the expected load characteristics [20] or classifying the users based on their load characteristics for "effective guidance electric energy conservation as well as to better realize peak load shifting" [21]. Some studies go even further and aim at a

specific topic—for example, shipboard microgrid load characteristics determination [22]. The IEC Smart Grid Standardization Roadmap tells us that there are many innovations on the way, many of which are part of the small electrical device category [23]. Some papers, such as [24–27], deal with these issues, but the load frequency characteristics are often missing. Most actual results are used in modern grid studies such as [28–33]. It is of the utmost importance to carry on contingency analyses, static and dynamic stability, and other frequency control studies [34–38]. This is also connected with the implementation of energy storage systems [39,40], expected rapid electromobility growth [41,42], and demand response management [43,44]. This paper aims to be another important update in terms of the smaller electrical loads and their frequency characteristics, which is an important baseline for many substantial safety and operation studies of the grid.

2. Measurement and Data Analysis

Load-frequency characteristics of single-phase home appliances specified in Table 1 were measured. They can be further categorized as follows Table 2:

- General categorization:
  - resistive loads (R);
  - motoric loads (M);
  - loads with electronic ballast (EB);
  - loads with magnetic ballast (MB).
- Light sources:
  - light sources with magnetic ballast (LM);
  - light sources with electronic ballast (LE);
  - resistive light sources (LR).

Table 1. List of measured single-phase home appliances.

Device	Nominal Power [W]	Reference	Remark and Operation Modes
Linear Fluorescent Lamp	36.0	Ballast: Helvar 36 A-T, Capacitor: 4.5 µF ± 10% Lamp: Osram Dulux L 36 W/840	Magnetic Ballast
High-Pressure Sodium Lamp A	70.0	Ballast: Helvar NK 70 LUP, Capacitor: 12 µF ± 10% Lamp: Osram VIALOX NAV(SON)-T 70 W 4Y	Magnetic Ballast
High-Pressure Sodium Lamp B	100.0	Ballast: Helvar NK 100 LUP, Capacitor: 12 µF ± 10% Lamp: Osram VIALOX NAV-T 100 W Super 4Y	Magnetic Ballast
Compact fluorescent Lamp	15.0	GM Electronic, Spiral 15 W	Electronic Ballast
LED Lamp A	50.0	Driver: Optotronic OT FIT 75/220–240/550 D LT2 LED: Acemi 0167	Nondimmable
openLED Lamp B	55.0	Cityled, CL 17–55 W B	Nondimmable
Wi-Fi Router	8.0	MSI, RG54G3	No PC Connected
LCD Monitor 17″	33.0	Philips 170B5	White Screen
CRT Television 28″	85.0	Philips, 28PT4475/58	White Noise screen
Video Projector	300.0	Benq, MP670	(Metal Halide Lamp) White Screen
Small Speakers	1.5	Genius, SP-Q06	White Noise Sound
Incandescent Lamp	25.0	Tesla, 741	Resistive light sources
Microwave	1200.0	Daewoo, KOG-370AA	Microwave 800 W; Grill 1050 W (operated at maximum microwave); stand by
Heat Gun	2000.0	Parkside, PHLG 2000 E4	–
Vacuum Cleaner	800.0	Sencor, SVC 730RD	–
Refrigerator	100.0	Calex, C275.1/6829	Operated After Long Downtime
Air Conditioner	1350.0	Comfee, MPD1–12CRN1	–
Rod Mixer A	600.0	Silvercrest, SSM 300 A1	No Load
Rod Mixer B	300.0	Bosch, MSM 66150	No Load
Hair Dryer	1400.0	ETA, 432090000	–

All stated home appliances have nominal voltage of 230 V, 50 Hz.

Table 2. List of categorizations of measured home appliances.

Device	General Categorization	Light Source Category
Linear Fluorescent Lamp	MB	LM
High-Pressure Sodium Lamp A	MB	LM
High-Pressure Sodium Lamp B	MB	LM
Compact fluorescent Lamp	EB	LE
LED Lamp A	EB	LE
LED Lamp B	EB	LE
Wi-Fi Router	EB	–
LCD Monitor 17″	EB	–
CRT Television 28″	EB	–
Video Projector	EB	–
Small Speakers	EB	–
Microwave—stand by	EB	–
Incandescent Lamp	R	LR
Microwave	R	–
Heat Gun	R	–
Vacuum Cleaner	M	–
Refrigerator	M	–
Air Conditioner	M	–
Rod Mixer A	M	–
Rod Mixer B	M	–
Hair Dryer	M	–

2.1. Measurement

The measurements aimed to analyze the behavior of household appliances when changing the frequency of the supply voltage. Measurement of frequency characteristics was performed in the range of 46.9 to 53.1 Hz. This range was chosen for the operation of on-grid and off-grid networks. To better capture the behavior of the appliances, they were measured from the lowest to the highest frequency, then repeated in reversed order, creating the full frequency range loop. The frequency step was 0.01 Hz and voltage was set to 230 V during all measurements. The workplace was fully automated for the repeatability of the measurements. The layout of the measuring apparatus is pictured in Figure 1.

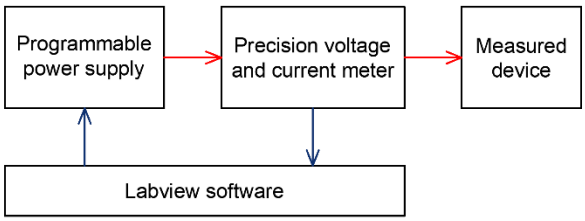

Figure 1. Measuring apparatus layout.

Each appliance measurement was performed by setting the value of frequency, stabilizing the observed properties, and then reading electrical parameters. Two types of cycles were realized: slow and fast. In the slow cycle, the stabilization time was 10 s, and in the fast cycle, it was 2 s. Specific time conditions during the measurement are pictured in Figure 2, which makes it possible to analyze the inertia of these devices. The chosen methodology is characterized by high measurement accuracy but lacks the versatility to measure all possible devices. Our measured appliances therefore needed to satisfy two conditions: (a) constant power consumption in a specified time; (b) primary usage in households. Such devices were selected and they are summarized in Table 1.

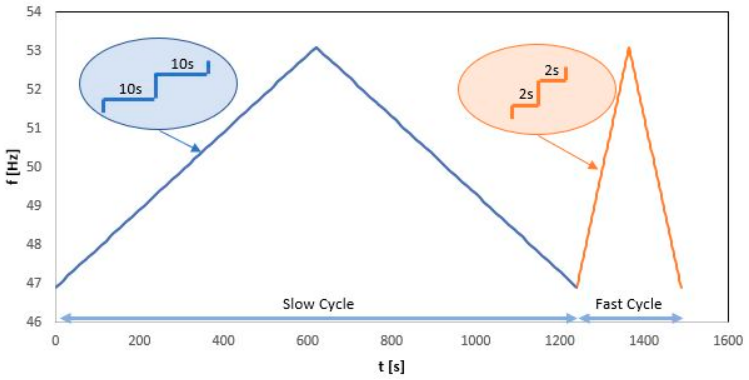

Figure 2. Specific time conditions during the measurement of selected devices.

The power supply was programmable AC source Chroma 61,505 with declared distortion under 0.3 at 50/60 Hz in connection with Reference Standard RS 3330E with maximum errors shown in Table 3.

Table 3. Maximum errors of measured values.

Value	Maximum Error
Voltage	0.0100%
Current	0.0100%
Active Power	0.0200%
Reactive Power	0.0200%
Apparent Power	0.0200%
Angle	0.0020°
Frequency	0.0001 Hz
Distortion	0.0050%

2.2. Data Analysis

Analyzed outputs of the measurement are values of active P and reactive power Q for each measured frequency and timestamp. Additional information from measurement is the total harmonic distortion of current (THDi) and power factor (PF). From this information, frequency bias factor (as stated in (1), generally defined as production and demand by the same manner) and frequency sensitivity coefficient (K_P), for all measured quantities, were calculated as stated in (2)–(5):

$$frequency\ bias\ factor\ K = \frac{\Delta P}{\Delta f} \tag{1}$$

$$frequency\ sensitivity\ coefficient\ K_P = \frac{\Delta P}{\Delta f}\frac{f_n}{P_n} \tag{2}$$

$$frequency\ sensitivity\ coefficient\ K_Q = \frac{\Delta Q}{\Delta f}\frac{f_n}{Q_n} \tag{3}$$

$$K_{THDi} = \frac{\Delta P}{\Delta f}\frac{f_n}{THDi_n} \tag{4}$$

$$K_{PF} = \frac{\Delta PF}{\Delta f}\frac{f_n}{PF_n} \tag{5}$$

where:

f [Hz]—frequency;

n [−]—index of nominal, reference, per unit, value of P, Q, $THDi$ and PF nominal frequency f_n 50 [Hz].

The frequency sensitivity coefficient K_P was evaluated as the linear regression slope calculated from measured scattered data of each quantity as a function of frequency. The

frequency interval 48–52 Hz was selected for evaluation due to the linearity of measured data in the interval. In practice, the devices also do not operate outside the selected frequency range. In general, the frequency sensitivity coefficient can be calculated without the application of per unit. However, it is necessary to use per unit values for comparison of different nominal power home appliances. Additionally, the frequency sensitivity coefficient without per unit frequency K_{fP} was calculated by altering Equation (2) resulting in Equation (6).

$$K_{fP} = \frac{\Delta P}{\Delta f} \frac{1}{P_n} \tag{6}$$

The same applies to other quantities such as Q, $THDi$, and PF, using altered versions of Equations (3)–(5) in a similar manner. Figures 3 and 4 show examples of analyzed K_P and K_{fP} obtained by (2), (5) and (6). Figures 5 and 6 represent all analyzed coefficients for Wi-Fi router as an example. In every case, the root mean square deviation (RMSD) was evaluated as well. RMSD is commonly used to evaluate the difference between measured and predicted data. In our case, the prediction is represented by a linear regression.

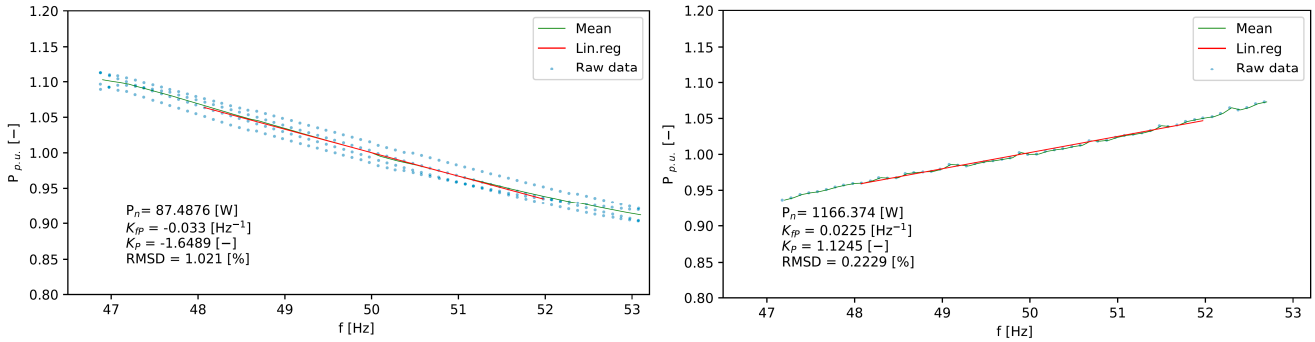

(**a**) (**b**)

Figure 3. Example of the analyzed result of static load characteristic of (**a**) high-pressure sodium Lamp (70 W); (**b**) microwave with grill (1050 W)

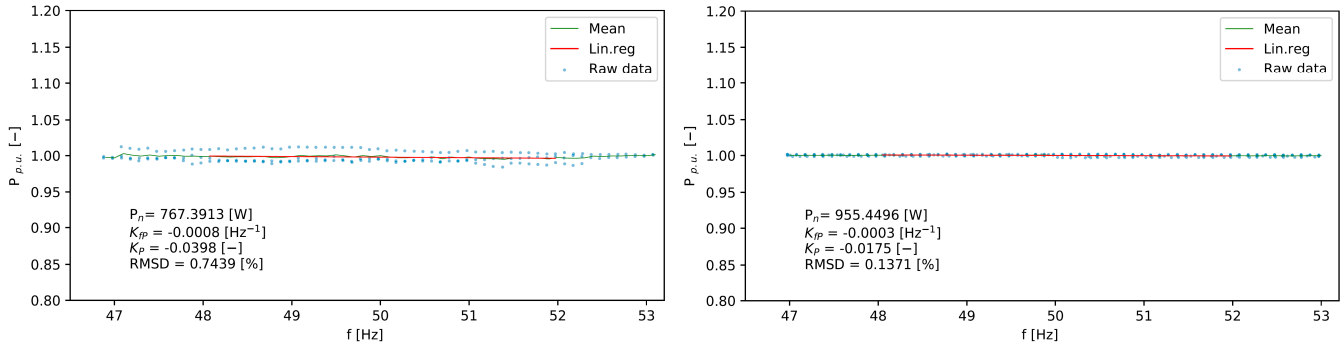

(**a**) (**b**)

Figure 4. Example of the analyzed result of static load characteristic of (**a**) vacuum cleaner (800 W); (**b**) and heat gun (2000 W) operated at half power.

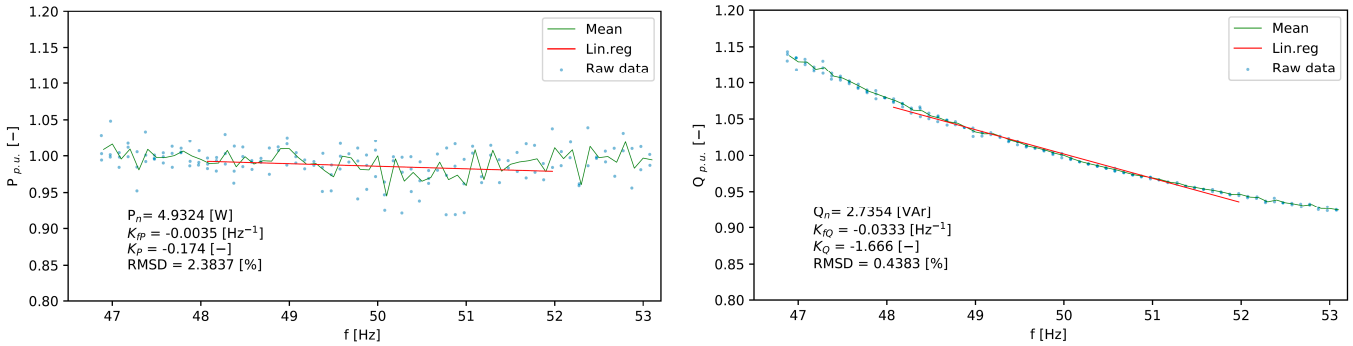

(**a**) (**b**)

Figure 5. Example of the analyzed characteristics of Wi-Fi router (**a**) K_P, K_{fP}; (**b**) K_Q, K_{fQ}.

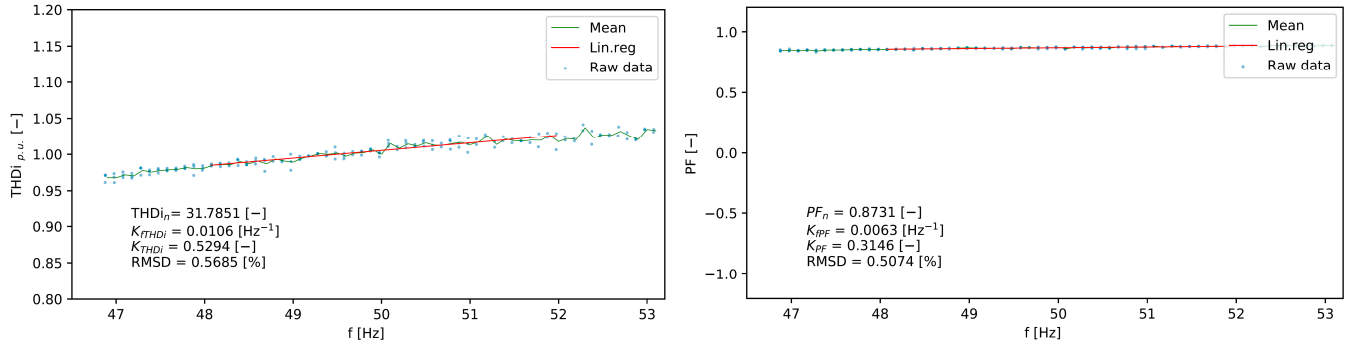

(**a**) (**b**)

Figure 6. Example of the analyzed characteristics of Wi-Fi router. (**a**) K_{fTHDi}, K_{THDi}; (**b**) K_{fPF}, K_{PF}.

3. Measurement Results

Tables 4 and 5 show the results of chosen parameters related to analyses of static frequency characteristics. Furthermore, they compare them by general categorization. Results in Table 4 refer to the evaluation of K_P and K_{THDi}, while results in Table 5 show K_Q and K_{PF} results. In all cases, the nominal (50 Hz) value of the quantity is stated along with RMSD. Based on the results, analyzed home appliances can be sorted according to the size of the frequency sensitivity coefficient value (Table 4):

- positive: $K_P > 0.01$;
- negative: $K_P < -0.01$;
- no effect (negligible): $-0.01 \leq K_P \leq 0.01$.

Table 4. Results of analyzed single-phase home appliances.

Device	Measured Active Power [W]	K_P [-]	RMSD [%]	Measured *THDi* [-]	K_{THDi} [-]	RMSD [%]	Reg. Effect
Linear Fluorescent Lamp	43.81	−1.29	0.26	22.19	0.09	0.48	Neg
High-Pressure Sodium Lamp A	87.49	−1.65	1.02	7.06	−1.46	2.87	Neg
High-Pressure Sodium Lamp B	107.60	−1.96	1.42	17.31	0.00	1.35	Neg
Compact Fluorescent Lamp	13.52	0.08	0.73	75.27	0.17	0.15	Pos
LED Lamp A	49.50	0.00	0.08	14.3	−0.10	0.50	no
LED Lamp B	56.00	0.00	0.11	5.81	0.68	1.44	no
Wi-Fi Router	4.93	−0.17	2.38	31.79	0.53	0.57	Neg
LCD Monitor 17″	25.42	−0.04	0.81	88.97	0.00	0.15	Neg
CRT Television 28″	53.81	0.04	0.80	88.00	−0.01	0.11	Pos
Video Projector	268.95	0.00	0.11	7.46	−1.03	1.40	no
Small Speakers	1.43	0.01	1.43	95.71	−0.01	0.06	no
Microwave—stand by	2.06	−2.61	0.93	46.57	−0.97	0.19	Neg
Incandescent Lamp	25.54	−0.01	0.09	1.12	−0.93	0.50	no
Microwave	1174.22	1.02	0.26	22.29	−3.91	0.65	Pos
Heat Gun	955.45	−0.02	0.14	0.57	0.20	3.15	Neg
Vacuum Cleaner	767.39	−0.04	0.74	5.95	0.05	0.91	Neg
Refrigerator	113.03	0.41	0.41	9.43	0.22	0.36	Pos
Air Conditioner	1121.09	0.79	0.10	17.18	−3.69	0.59	Pos
Rod Mixer A	5.96	−1.05	1.91	95.30	0.09	0.16	Neg
Rod Mixer B	28.84	−0.13	0.57	77.37	−0.03	0.11	Neg
Hair Dryer	590.07	0.18	1.84	25.76	−0.58	4.52	Pos

Orange—MB (magnetic ballast), Blue—EB (electronic ballast), Red—R (resistive), and Green—M (motor).

Table 5. Results of analyzed single-phase home appliances.

Device	Measured Reactive Power [VAr]	K_Q [-]	RMSD [%]	Measured PF [-]	K_{PF} [-]	RMSD [%]
Linear Fluorescent Lamp	16.55	−10.72	3.33	0.94	1.10	0.45
Hight Pressure Sodium Lamp A	209.51	−0.79	1.21	0.39	−0.28	0.72
Hight Pressure Sodium Lamp B	74.64	−5.90	5.07	0.82	1.05	1.69
Compact fluorescent Lamp	−18.34	0.29	0.72	0.59	−0.08	0.09
LED Lamp A	−16.00	0.51	0.10	0.95	−0.05	0.01
LED Lamp B	−19.22	0.86	0.17	0.95	−0.09	0.02
Wi-Fi Router	2.74	−1.67	0.44	0.87	0.31	0.51
LCD Monitor 17″	−53.16	0.02	0.44	0.43	−0.02	0.29
CRT Television 28″	−101.39	−0.04	0.43	0.47	0.03	0.18
Video Projector	−36.57	−0.01	0.65	0.99	0.00	0.01
Small Speakers	−4.76	−0.12	0.88	0.29	0.03	0.18
Microwave—stand by	3.30	−7.39	1.75	0.53	1.81	0.33
Incandescent Lamp	−0.40	−0.99	0.27	1.00	0.00	0.00
Microwave	334.43	−8.12	2.53	0.96	0.67	0.30
Heat Gun	−5.73	0.10	1.06	1.00	0.00	0.00
Vacuum Cleaner	108.24	0.74	0.81	0.99	−0.01	0.02
Refrigerator	122.54	−0.94	0.12	0.68	0.50	0.15
Air Conditioner	190.50	−10.35 (47–50.2 Hz) −101.52 (50.2–51 Hz) −1.99 (50.5–51 Hz)	1.16 (47–50.2 Hz) 13.97 (50.2–51 Hz) 0.55 (50.5–51 Hz)	0.98	0.18	0.22
Rod Mixer A	20.74	−0.38	1.35	0.28	−0.17	0.17
Rod Mixer B	5.05	−22.72	119.83	0.63	0.02	0.07
Hair Dryer	−121.02	1.35	14.57	0.90	0.15	1.60

Orange—MB (magnetic ballast), Blue—EB (electronic ballast), Red—R (resistive), and Green—M (motor).

The graph in Figure 7 shows a comparison of analyzed single-phase home appliances with a negative value of frequency sensitivity coefficient K_P. These devices increase the active power consumption with a positive change in frequency and thus counteract the character of frequency control (production/generator control). The frequency control character is also determined by the frequency sensitivity coefficient or, in other words, the sum of the coefficients of the generators involved in the frequency control. In this case, the system (control area) must have a control reserve to maintain the required frequency value for contingency situations. The next graph shows the measured loads with a positive value of frequency sensitivity coefficient K_P. These devices work in conjunction with the frequency control (production/generator control)—i.e., devices positively affect frequency control because of self-regulating behavior. A comparison of the measured light sources is shown in Table 6. The evaluation of the measured loads showed in one case a certain interest in comparison with other loads. As shown in Table 5, the air conditioner has three different K_Q, which differs by frequency range. This is because the static characteristic is not linear (Figure 8).

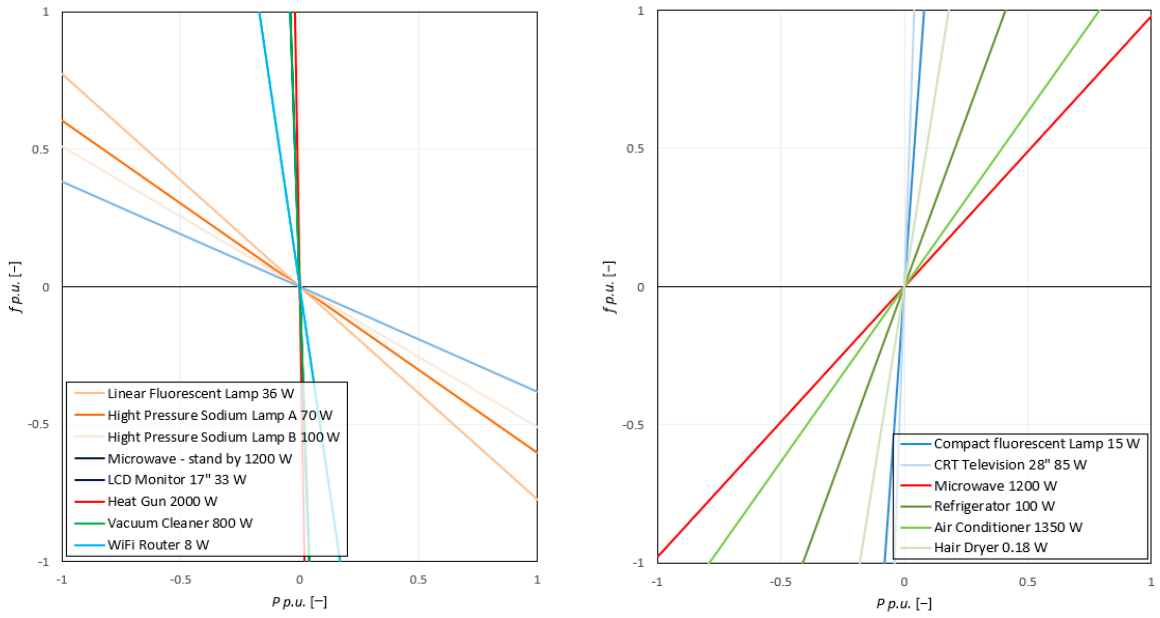

(**a**) (**b**)

Figure 7. Graphical comparison of analyzed single-phase appliances according to the value of frequency sensitivity coefficient (**a**) negative: $K_P < -0.01$; (**b**) positive: $K_P > 0.01$.

Table 6. Comparison of light sources.

Device	K_P [-]	K_Q[-]	K_{THDi} [-]	K_{PF} [-]	Light Source Category
Linear Fluorescent Lamp	−1.29	−10.72	0.09	1.10	Light sources with magnetic ballast
High-Pressure Sodium Lamp A	−1.65	−0.79	−1.46	−0.28	
High-Pressure Sodium Lamp B	−1.96	−5.90	0.00	1.05	
Compact fluorescent Lamp	0.08	0.29	0.17	−0.08	Light sources with electronic ballast
LED Lamp A	0.00	0.51	−0.10	−0.05	
LED Lamp B	0.00	0.86	0.68	−0.09	
Incandescent Lamp	−0.01	−0.99	−0.93	0.00	Resistive light sources

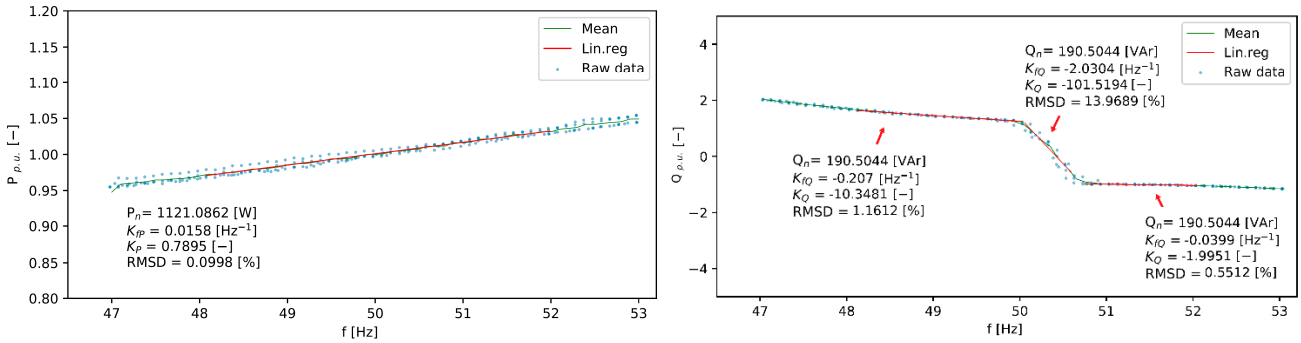

Figure 8. Analyzed load static characteristics of air conditioner (**a**) K_P, K_{fP} ; (**b**) K_Q, K_{fQ} .

Discussion on Measurement Results

In the field of load modeling, research and analysis of static characteristics have been published in a relatively large number of studies. Some studies were aimed at evaluating the frequency sensitivity coefficients K_P and K_Q. Comparison of these coefficients for selected devices is shown in Table 7 based on three different literature sources, including our measurement. For the coefficient K_P, it can be concluded that the results are almost the same for stated devices—i.e., the effect on frequency control is the same. For the coefficient K_Q, it can be stated that the results differ significantly in size in some cases, but the character of the reactive power change with the frequency change remains the same. From the available information, it is not possible to quantify the cause of these differences.

Table 7. Comparison of the frequency sensitivity coefficient based on 3 different literature sources.

Device	K_P [-]			K_Q [-]			PF [-]		
Incandescent lights	0.00	0.00	−0.01	0.00	0.00	−0.99	1.00	1.00	1.00
Television	0.00	0.00	0.04	−4.50	−2.60	−0.04	0.80	-	0.47
Heat Gun	-	0.00	−0.02	-	0.00	0.10	-	1.00	1.00
Refrigerator	0.53	0.50	0.41	−1.50	−1.40	−0.94	0.80	0.79	0.68
Air Conditioner	0.98	0.90	0.79	−1.30	−2.70	−10.35 (47–50.2 Hz) −101.52 (50.2–51 Hz) −1.99 (50.5–51 Hz)	0.90	0.97	0.98

Blue—OMARA, H. "A Methodology for Determining the Load Frequency Sensitivity." The thesis for a of Doctor of Philosophy degree, The University of Manchester, England—Manchester, December 2012 [8]. Red—Concordia, C., and S. Ihara. "Load Representation in Power System Stability Studies." IEEE Transactions on Power Apparatus and Systems PAS-101, no. 4 (April 1982) [6]. Green—our measurement results.

Based on the above, the common negative side of different studies is the unspecified methodology of measuring selected electrical variables of devices. This factor could ultimately cause differences in the results for determining the static characteristics. Therefore, the following factors should be considered in order to correct the classification of the devices (or to divide the equipment according to the frequency sensitivity coefficient) in terms of the effect on the frequency change:

- Measurement methodology:
  - frequency range (minimum proposed range between 47.5 and 51.5 Hz due to requirements on generating modules [45]);
  - equipment stabilization (e.g., thermal, . . .).
- Defined operating conditions of the device:
  - stand-by mode;
  - no-load;
  - load level (average, max, . . .).

The results shown in Table 8 confirm the operation conditions of the device can significantly affect the incorrect determination of the coefficients K_P and K_Q. This influence can be even more pronounced when solving, e.g., dynamic simulations with frequency deviations.

Table 8. Comparison of the frequency sensitivity coefficient of microwave—different operation conditions.

Device	K_P [-]	K_Q [-]	PF [-]
Microwave—stand by	−2.61	−7.39	0.53
Microwave	1.02	−8.12	0.96

4. Impact of Measured Loads on Frequency Control in Island Operation

To assess the impact on frequency control in island operation, we considered a block diagram of the load-frequency control for a simple single machine system, also known as single input-single output system in case of a production outage of 10%. The control scheme used for the simulations is shown in Figure 9. In this case, the machine model considers a turbine used for frequency control—i.e., a simplified simulation model of frequency control is assumed.

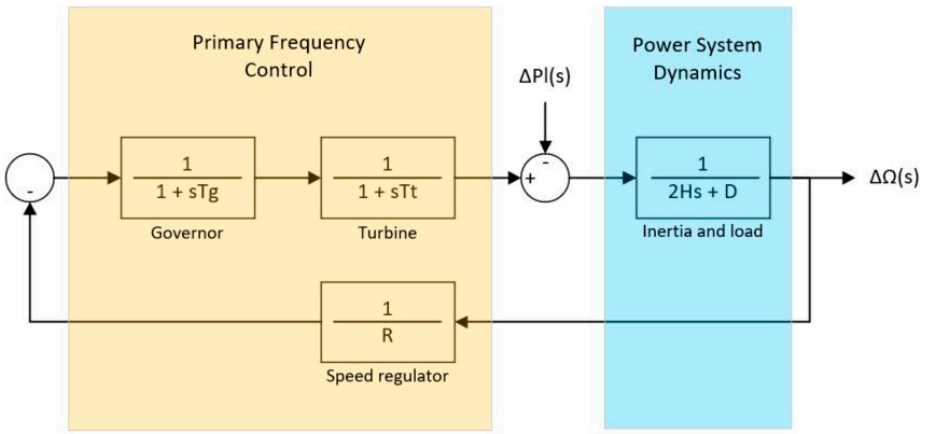

Figure 9. Primary frequency control scheme used for simulations [3].

The isolated island operation had the following parameters:

- turbine time constant (Tt) = 0.5 s;
- governor time constant (Tg) = 0.2 s;
- governor speed regulator (droop characteristic) (R) = 5%;
- inertia time constant (H) = 5 s;
- damping constant (D) (or K_P for load—measured device);
- power load change (ΔPl) = −10% (generation outage).

Furthermore, we considered measured data of simple appliances divided into three categories according to the frequency sensitivity coefficient. The simulations were performed for each separately measured device—i.e., the total load in island operation was always characteristic for only one device. Within the simulations, we only considered the primary frequency control (without automatic generation control) as a sufficient approach to frequency deviation assessment. The closed-loop transfer function relating the fixed generation step change, $-\Delta Pl(s)$, which is commonly assumed for the frequency control to the angular frequency deviation from the nominal reference (50 Hz), $\Delta\Omega(s)$, can be defined according to Figure 10 as (7) or (8):

$$\frac{\Delta\Omega(s)}{-\Delta Pl(s)} = T(s) = \frac{(1+Tgs)(1+Tts)}{(2Hs+K\_P)(1+Tgs)(1+Tts)+\frac{1}{R}} \quad (7)$$

$$\Delta\Omega(s) = -\Delta Pl(s)T(s) \tag{8}$$

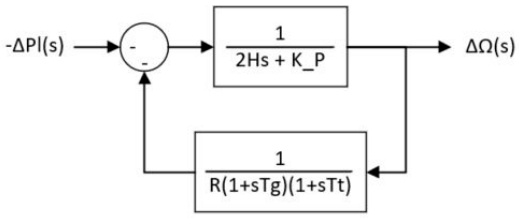

Figure 10. Load frequency control diagram with input $\Delta Pl(s)$ and output $\Delta\Omega(s)$.

Then, we can consider the generation change as a step input:

$$-\Delta Pl(s) = \frac{-\Delta Pl}{s} \tag{9}$$

Utilizing the final value theorem, the steady state value of $\Delta\omega$ and value of quasi-stationary deviation Δf can be calculated by the following procedure:

$$\Delta\omega = \lim_{s\to 0} s\Delta\Omega(s) = (-\Delta Pl)\frac{1}{K\_P + \frac{1}{R}} \tag{10}$$

$$\Delta f = \Delta\omega f_n \tag{11}$$

To obtain the value of maximum (dynamic) frequency deviation Δf_{max}, it is necessary to evaluate the results of a step response of dynamic system (concerning generation change of -10%) represented by the transfer function determined for every measured device as follows:

$$T(s) = \frac{(1+Tgs)(1+Tts)}{(2Hs+K\_P)(1+Tgs)(1+Tts)+\frac{1}{R}} \tag{12}$$

$$T(s) = \frac{quadratic\ \text{polynomial}}{cubic\ \text{polynomial}} \tag{13}$$

4.1. Discussion on Simulation Results

The results of simulations were performed for each load with the evaluation of the following quantities:

- maximum (dynamic) frequency deviation (Δf_{max});
- quasi-stationary deviation (Δf).

The results in Table 9 confirm the influence assumption of the frequency sensitivity coefficient of particular loads on the magnitude of the dynamic and quasi-stationary frequency deviation during the primary frequency control in island operation. Graphs of frequency responses measured by home appliances are shown in Figure 11. The frequency response for devices without significant influence can be considered a reference waveform within the mutual comparison. For devices with a negative frequency sensitivity coefficient, a more significant decrease in frequency is evident after production outage. These devices aggravate the effect of primary frequency control. Conversely, for devices with positive frequency sensitivity coefficients, the frequency deviations were lower. These devices derive the primary frequency control—i.e., their behavior during the frequency change improves the effect on the frequency control. On the other hand, it is necessary to emphasize that to know or evaluate the state frequency sensitivity coefficients K_P and K_Q could be considered as generally insufficient due to the natural behavior of electricity demand typical of its dynamic over time in terms of magnitude. However, we can state that it is sufficient to determine a valuable estimation in load-frequency sensitivity.

Table 9. Simulation results after production outage of 10% considering chosen appliances as only load.

Device	K [W/Hz]	K_P [-]	Δfmax [Hz]	Δf [Hz]	Reg. Effect
Linear Fluorescent Lamp	−1.126	−1.290	−0.425	−0.267	Neg
High-Pressure Sodium Lamp A	−2.885	−1.650	−0.436	−0.272	Neg
High-Pressure Sodium Lamp B	−4.209	−1.960	−0.446	−0.277	Neg
Wi-Fi Router	−0.017	−0.170	−0.395	−0.252	Neg
LCD Monitor 17″	−0.020	−0.040	−0.392	−0.251	Neg
Microwave—stand by	−0.107	−2.610	−0.467	−0.288	Neg
Heat Gun	−0.334	−0.020	−0.391	−0.250	Neg
Vacuum Cleaner	−0.610	−0.040	−0.392	−0.251	Neg
Rod Mixer A	−0.125	−1.050	−0.419	−0.264	Neg
Rod Mixer B	−0.076	−0.130	−0.394	−0.252	Neg
LED Lamp A	0.001	0.000	−0.391	−0.250	no
LED Lamp B	−0.002	0.000	−0.391	−0.250	no
Video Projector	−0.003	0.000	−0.391	−0.250	no
Small Speakers	0.000	0.010	−0.391	−0.250	no
Incandescent Lamp	−0.005	−0.010	−0.391	−0.250	no
Compact fluorescent Lamp	0.022	0.080	−0.389	−0.249	Pos
CRT Television 28″	0.041	0.040	−0.390	−0.250	Pos
Microwave	23.920	1.020	−0.367	−0.238	Pos
Refrigerator	0.929	0.410	−0.381	−0.245	Pos
Air Conditioner	17.701	0.790	−0.372	−0.241	Pos
Hair Dryer	2.150	0.180	−0.387	−0.25	Pos

4.2. Concerning Further Smart Grid Possibilities

The simulation results above confirmed that the dynamic frequency deviation and the quasi-stationary load-frequency dependence in island operation could be more significant than in large power systems. In the case of droop-based frequency control of the generation, the load-frequency dependence influences the steady-state operating point. This type of frequency control assumes the share of resources with inertia. Therefore, a methodology for determining frequency-dependent characteristics of loads is necessary for such smart grid systems. However, this scenario may face new technical challenges from the growing number of loads and generation based on power electronics. Synchronous generators are likely to be largely replaced by inverter-based technologies, which means loss of or reduction in inertia. Potential disturbances in such systems can cause significant frequency and voltage instability, leading to local blackouts in island operations. Consequently, the restoration of such systems will probably not be able to be autonomous.

Other approaches to frequency control must be considered in the case of a large share of renewables in the smart grid energy mix with a small inertia effect. A potential solution for improving frequency stability with small inertia due to many inverters on the production side is to fortify the system with virtual inertia. These virtual systems can be established using an energy storage system and power electronics in order to meet the requirements of a sufficient inertia value and avoid the high-frequency deviations. In any case, both scenarios prove that probably the most important parameter for achieving long-term stability in real operation is the presence of inertia. The same applies to the current power system and will apply to future systems and island smart grids. On this basis, the need to consider the static load characteristics for the operation planning of smart grid regions is again emphasized. This methodology will also be important for assessing the ability to operate such a smart grid. Accurate modeling of the load will have an important role in analyzing the frequency stability of the power system. Before modeling, the particular devices must be properly measured and their impacts correctly verified. Subsequent faithful reproductions of the accurate responses of the devices will be a big challenge due to the diversity of loads in distribution systems.

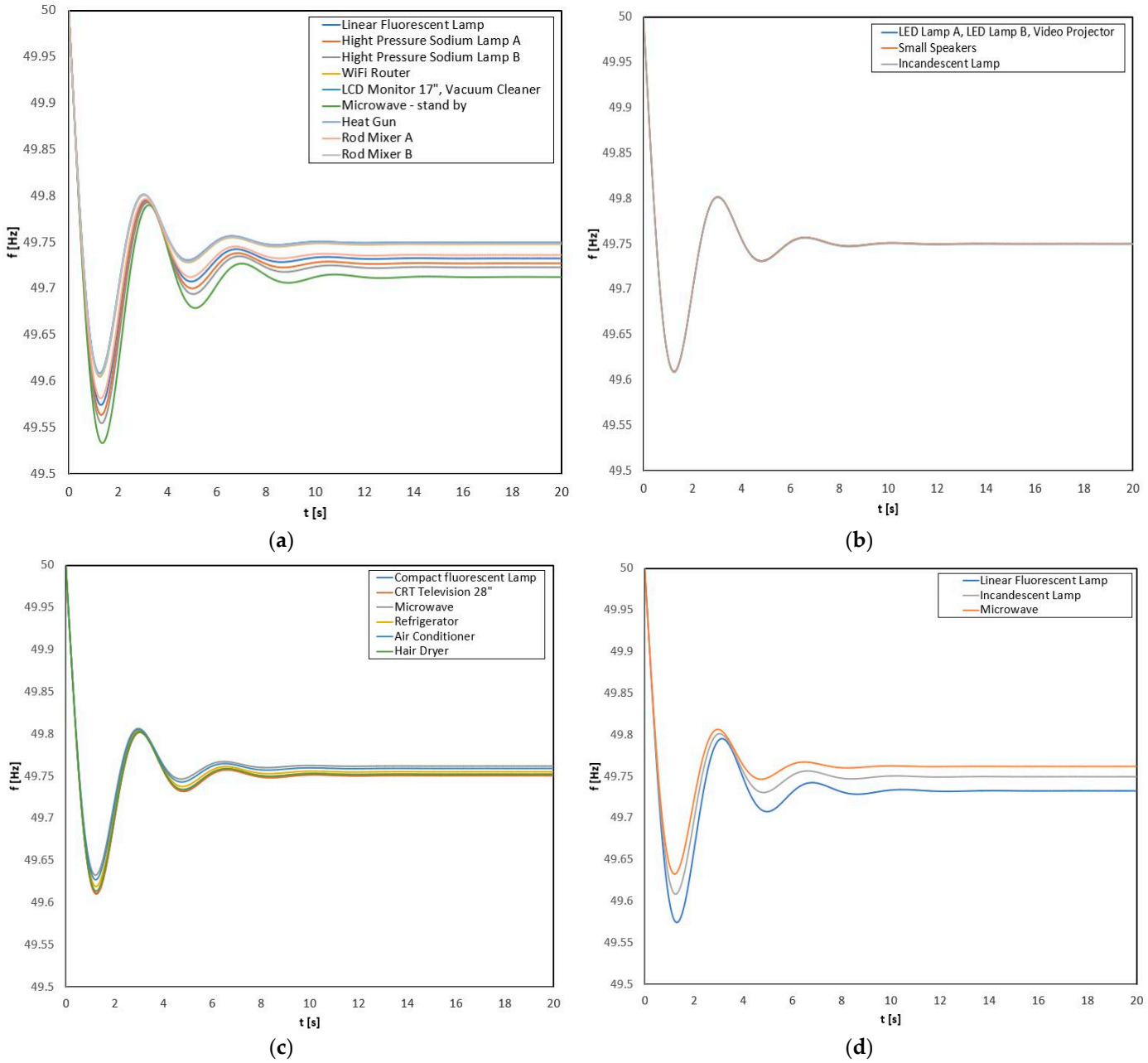

Figure 11. Frequency response after production outage of 10% considering chosen appliances as loads only with (**a**) negative effect; (**b**) no effect; (**c**) positive effect; (**d**) comparatively different effects.

5. Conclusions

This work aimed to measure selected devices commonly used at home or work (simple single-phase home appliances) to evaluate the static frequency characteristics of these devices. These devices were divided into two groups: general and light sources. The following parameters were measured for each device with a frequency step of 0.01 Hz: *P*, *Q*, *THDi*, and PF. Subsequently, the following frequency sensitivity coefficients were evaluated: K_P, K_Q, K_{THDi} and K_{PF}. Based on the results, analyzed home appliances were sorted into three categories according to the size of their frequency sensitivity coefficient values: positive, negative, and no effect (negligible).

The shown results were compared with studies aimed at evaluating the static load characteristics. For the coefficient K_P, the results are comparable (almost the same), but for the coefficient K_Q, the results are more variable and, in some cases, significantly different.

From the available information, it is not possible to quantify the cause of these differences. The comparison confirmed the need to define a uniform measurement methodology (frequency range and equipment/device stabilization condition during the measurement). In this context, there is also a uniform definition of operating conditions of the device to determine the frequency sensitivity coefficient. This requirement is essential, and confirmed our evaluation of the microwave device. In normal operation, the coefficient K_P had a positive value and a negative value in standby mode. The available studies on this issue do not provide any additional information on the measurement method, and only the results are available. For this reason, it is not possible to make a correct comparison. However, it can be stated that the results have the same characteristics. Further, the evaluated frequency sensitivity coefficient was used to assess the impact of measured devices on frequency control in island operation. During the island operation, droop-based frequency control of the generation and a production outage of 10% were considered. The results confirmed the influence assumption of the frequency sensitivity coefficient of particular loads on the magnitude of the dynamic and quasi-stationary frequency deviation during the primary frequency control in island operation. Devices/loads may have either stabilizing or destabilizing effects depending on the static frequency characteristic. It has been shown that system stability can increase with higher positive frequency sensitivity coefficient K_P values and decreased with lower negative values. It has also been shown that the static load characteristic can have a decisive influence on the system frequency instability, especially in small island operation or a smart grid system. The available studies [6,8,28] on frequency response indicate the same results. Based on the above, it is clear that static load characteristics in simulation calculations are significant. In order to achieve correct frequency response results, it is necessary to have the correct input data. Therefore, these characteristics must be measured and evaluated with sufficient accuracy.

There are several areas where further research is needed, including:

- identification and organization of more data of household appliances in more detail and, if possible, creation of common data groups so that that load group composition may be estimated more easily and reliably;
- measurement of static load characteristics of a wider group of the same type of devices (improvement of current statistics and addition of new types of loads);
- measurement of static characteristics of three-phase devices (a wider group of devices);
- analysis of the frequency response in island operation concerning a larger number of devices with different frequency sensitivity coefficients;
- focusing on devices with reactive power consumption—the operating impedance is frequency-dependent.

Author Contributions: Conceptualization, A.B., B.C., P.J., Ž.E. and A.Š.; Formal analysis, M.C. and J.B.; Funding acquisition, A.B.; Investigation, M.C., J.B. and B.C.; Methodology, A.B., B.C., J.B., Ž.E. and A.Š.; Project administration, A.B.; Software, M.C., P.J., B.C. and J.B.; Supervision, A.B.; Validation, M.C., P.J. and J.B.; Visualization, M.C., P.J. and J.B.; Writing—original draft, B.C., M.C., P.J. and J.B.; Writing—review and editing, A.B., M.C. and J.B. All authors have read and agreed to the published version of the manuscript.

Funding: This paper was supported by the agency VEGA MŠVVaŠ SR under Grant No. 1/0640/17 "Smart Grids, Energy Self-Sufficient Regions and their Integration in Existing Power System".

Institutional Review Board Statement: Not applicable.

Informed Consent Statement: Not applicable.

Data Availability Statement: Data is contained within the article.

Acknowledgments: We would like to thank the Applied Precision Ltd. Company for renting out the device Reference Standard RS 3330E for free. The device was used for measuring of the frequency characteristics of appliances concerning this project—appliedp.com.

Conflicts of Interest: The authors declare no conflict of interest.

References

1. Hoballah, A. *Power System Stability Assessment and Enhancement Using Computational Intelligence*; Universität Duisburg-Essen: Duisburg, Germany, 2011.
2. Machowski, J.; Lubosny, Z.; Bialek, J.W.; Bumby, J.R. *Power System Dynamics: Stability and Control*; John Wiley & Sons: Hoboken, NJ, USA, 2020; ISBN 978-1-119-52634-6.
3. Kundur, P. *Power System Stability and Control*; McGraw-Hill: New York, NY, USA, 1994; ISBN 978-0-07-063515-9.
4. Shenkman, A.L. *Transient Analysis of Electric Power Circuits Handbook*; Springer Science & Business Media: New York, NY, USA, 2006; ISBN 978-0-387-28799-7.
5. Load Representation for Dynamic Performance Analysis (of Power Systems). *IEEE Trans. Power Syst.* **1993**, *8*, 472–482. [CrossRef]
6. Concordia, C.; Ihara, S. Load Representation in Power System Stability Studies. *IEEE Trans. Power Appar. Syst.* **1982**, *PAS-101*, 969–977. [CrossRef]
7. O'Sullivan, J.; Power, M.; Flynn, M.; O'Malley, M. Modelling of Frequency Control in an Island System. In Proceedings of the IEEE Power Engineering Society 1999 Winter Meeting (Cat. No.99CH36233), New York, NY, USA, 31 January–4 February 1999; Volume 1, pp. 574–579.
8. Omara, H. A Methodology for Determining the Load Frequency Sensitivity. Ph.D. Thesis, The University of Manchester, Manchester, UK, 2012.
9. Azizan, A.R.B. *Simulation of Dynamic Load Effect on Power System*; Universiti Tun Hussein Onn Malaysia: Parit Raja, Malaysia, 2013.
10. Abhyankar, S.; Balasubramaniam, K.; Cui, B. Load Model Parameter Estimation by Transmission-Distribution Co-Simulation. In Proceedings of the Power Systems Computation Conference (PSCC), Dublin, Ireland, 11–15 June 2018; pp. 1–7.
11. Bevrani, H.; Shafiee, Q.; Golpira, H.; Taczi, I.; Hartmann, B.; Vokony, I.; Lak, M.; Aragon, E.; Johnson, A.; Russell, B.; et al. *Smart Grid and Stability of Power Systems*; IEEE Smart Grid Recource Center: New York, NY, USA, 2019.
12. Sabbir, K.G.; Kashem, M.A.; Negnevitsky, M. Response Analysis of Large Induction Motors at Different Voltages and Frequencies. In Proceedings of the Australasian Universities Power Engineering Conference (AUPEC 2006), Melbourne, Australia, 10–13 December 2006.
13. Chen, Q.; Jiang, M.; Ju, P.; Shan, X.; Wang, B.; Wang, Y.; Yu, F.; Xu, L.; Qin, C. Frequency Characteristic of New-Type Load Considering Power Electronics Technology. In Proceedings of the IEEE 7th Annual International Conference on CYBER Technology in Automation, Control, and Intelligent Systems (CYBER), Honolulu HI, USA, 31 July–4 August 2017; pp. 730–734.
14. Davidson, J.; Ringwood, J.V. Mathematical Modelling of Mooring Systems for Wave Energy Converters—A Review. *Energies* **2017**, *10*, 666. [CrossRef]
15. Lindén, K.; Segerqvist, I. *Modelling of Load Devices and Studying Load/System Characteristics*; School of Electrical and Computer Engineering, Chalmers University of Technology: Göteborg, Sweden, 1993.
16. Yamashita, K.; Djokic, S.; Matevosyan, J.; Resende, F.O.; Korunovic, L.M.; Dong, Z.Y.; Milanovic, J.V. Modelling and Aggregation of Loads in Flexible Power Networks—Scope and Status of the Work of CIGRE WG C4.605. *IFAC Proc. Vol.* **2012**, *45*, 405–410. [CrossRef]
17. Wang, Q.; Zhao, B.; Tang, Y.; Liu, L.-P. Modeling of Load Frequency Characteristics in the Load Model for Power System Digital Simulation. In Proceedings of the IEEE 7th Annual International Conference on CYBER Technology in Automation, Control, and Intelligent Systems (CYBER), Honolulu, HI, USA, 31 July–4 August 2017; pp. 538–542.
18. Changchun, C.; Yuqing, J.; Yiping, Y.; Ping, J. Load Modeling with Considering Frequency Characteristic. In Proceedings of the International Conference on Sustainable Power Generation and Supply (SUPERGEN 2012), Hangzhou, China, 8–9 September 2012; pp. 1–6.
19. Yamashita, K.; Asada, M.; Yoshimura, K. A Development of Dynamic Load Model Parameter Derivation Method. In Proceedings of the IEEE Power Energy Society General Meeting, Calgary, AB, Canada, 26–30 July 2009; pp. 1–8.
20. Lian, H.; Di, X.; Shen, Z.; Feng, M. Detailed Power Distribution Network Planning Based on the Description of Load Characteristics. In Proceedings of the China International Conference on Electricity Distribution (CICED), Shenzhen, China, 23–26 September 2014; pp. 1759–1762.
21. Diao, Y.; Liu, K.; Hu, L.; Jia, D.; Dong, W. Classification of Massive User Load Characteristics in Distribution Network Based on Agglomerative Hierarchical Algorithm. In Proceedings of the International Conference on Cyber-Enabled Distributed Computing and Knowledge Discovery (CyberC), Chengdu, China, 13–15 October 2016; pp. 169–172.
22. Chen, C.; Su, C.; Teng, J. Determination of Load Characteristics for Electrical Load Analysis in Shipboard Microgrids. In Proceedings of the IEEE/IAS 55th Industrial and Commercial Power Systems Technical Conference (I CPS), Calgary, AB, Canada, 5–8 May 2019; pp. 1–9.
23. IEC Smart Grid Standardization Roadmap. Available online: https://www.iec.ch/smartgrid/downloads/sg3_roadmap.pdf (accessed on 9 July 2020).
24. Zhang, Q.; Guo, Q.; Yu, Y. Research on the Load Characteristics of Inverter and Constant Speed Air Conditioner and the Influence on Distribution Network. In Proceedings of the China International Conference on Electricity Distribution (CICED), Xi'an, China, 10–13 August 2016; pp. 1–4.
25. Gong, C.; Zhang, B.; Ding, Y.; Ma, L.; Zhao, Y.; Li, X. Operating Characteristics and Influence on Power Grid with Distributed Electric Heating Considering Load Transfer. In Proceedings of the 2nd IEEE Conference on Energy Internet and Energy System Integration (EI2), Beijing, China, 20–22 October 2018; pp. 1–4.

26. Hou, P.; Wang, J.; Xu, Y.; Huang, K.; Li, J. Research on the Dynamic Characteristics of Microgrid with Pulsed Nonlinear Load. In Proceedings of the IEEE 8th International Power Electronics and Motion Control Conference (IPEMC-ECCE Asia), Hefei, China, 22–25 May 2016; pp. 1732–1736.
27. Yang, Y.; Liu, G.; Yang, Z.; Fan, S. A Study of Load Characteristic of the Building Heating and Cooling System in Smart Distribution Grid. In Proceedings of the China International Conference on Electricity Distribution (CICED), Shenzhen, China, 23–26 September 2014; pp. 928–932.
28. Huang, H.; Li, F. Sensitivity Analysis of Load-Damping Characteristic in Power System Frequency Regulation. *IEEE Trans. Power Syst.* **2013**, *28*, 1324–1335. [CrossRef]
29. Liao, S.; Xu, J.; Sun, Y.; Gao, W.; Ma, X.-Y.; Zhou, M.; Qu, Y.; Li, X.; Gu, J.; Dong, J. Load-Damping Characteristic Control Method in an Isolated Power System With Industrial Voltage-Sensitive Load. *IEEE Trans. Power Syst.* 2016. [CrossRef]
30. Obaid, Z.A.; Cipcigan, L.M.; Abrahim, L.; Muhssin, M.T. Frequency Control of Future Power Systems: Reviewing and Evaluating Challenges and New Control Methods. *J. Mod. Power Syst. Clean Energy* **2019**, *7*, 9–25. [CrossRef]
31. Popa, G.N.; Iagăr, A.; Diniș, C.M. Considerations on Current and Voltage Unbalance of Nonlinear Loads in Residential and Educational Sectors. *Energies* **2021**, *14*, 102. [CrossRef]
32. Saeed Uz Zaman, M.; Irfan, M.; Ahmad, M.; Mazzara, M.; Kim, C.-H. Modeling the Impact of Modified Inertia Coefficient (H) Due to ESS in Power System Frequency Response Analysis. *Energies* **2020**, *13*, 902. [CrossRef]
33. Järventausta, P.; Repo, S.; Rautiainen, A.; Partanen, J. Smart Grid Power System Control in Distributed Generation Environment. *IFAC Proc. Vol.* **2009**, *42*, 10–19. [CrossRef]
34. Steinhart, C.J.; Gratza, M.; Kerber, G.; Finkel, M.; Witzmann, R. Determination of Load-Frequency Dependence in Island Power Supply. *CIRED—Open Access Proc. J.* **2017**, *2017*, 1031–1034. [CrossRef]
35. Ulbig, A.; Borsche, T.S.; Andersson, G. Impact of Low Rotational Inertia on Power System Stability and Operation. *IFAC Proc. Vol.* **2014**, *47*, 7290–7297. [CrossRef]
36. Ye, L.; Baohui, Z.; Tingyue, T.; Zhe, G. Influence of Load Characteristics on System Dynamics and Load-Shedding Control Effects in Power Grid. In Proceedings of the 27th Chinese Control and Decision Conference (2015 CCDC), Qingdao, China, 22–25 May 2015; pp. 5160–5163.
37. Bracinik, P.; Latkova, M.; Altus, J. Retrofit of Distributed Generation vs. Frequency Control in Smart Grids at Overfrequency. *Electr. Eng.* **2017**, *99*, 1403–1415. [CrossRef]
38. Kanálik, M.; Margitová, A.; Dolník, B.; Medved', D.; Pavlík, M.; Zbojovský, J. Analysis of Low-Frequency Oscillations of Electrical Quantities during a Real Black-Start Test in Slovakia. *Int. J. Electr. Power Energy Syst.* **2021**, *124*, 106370. [CrossRef]
39. Vengatesh, R.P.; Rajan, S.E.; Sivaprakash, A. An Intelligent Approach for Dynamic Load Frequency Control with Hybrid Energy Storage System. *Aust. J. Electr. Electron. Eng.* **2019**, *16*, 266–275. [CrossRef]
40. Vrana, M.; Drapela, J.; Topolanek, D.; Vycital, V.; Jurik, M.; Blahusek, R.; Kurfirt, M. Battery Storage and Charging Systems Power Control Supporting Voltage in Charging Mode. In *Proceedings of the 19th International Conference on Harmonics and Quality of Power (ichqp), Dubai, United Arab Emirates, 6–7 July 2020*; IEEE: New York, NY, USA, 2020; ISBN 978-1-72813-697-4.
41. Ni, F.; Deng, C.; Wang, C.; Liu, Z. Research of Load Characteristics of Fast Charge for EVs. In Proceedings of the IEEE Conference and Expo Transportation Electrification Asia-Pacific (ITEC Asia-Pacific), Beijing, China, 31 August—3 September 2014; pp. 1–3.
42. Liu, M.; Zou, W.; Yang, M.; Huang, R.; Wei, S.; Yu, M. Analysis on Load Characteristics of Distributed Photovoltaic Access to EVs Industry. In Proceedings of the IEEE Sustainable Power and Energy Conference (iSPEC), Beijing, China, 20–24 November 2019; pp. 2547–2550.
43. Fan, L.; Jing, P.; Fubo, L.; Fuchao, L.; Xia, H.; Gang, Z. Research on Load Characteristic Modeling and Optimization Control Method Based on Demand Response. In Proceedings of the IEEE 4th Information Technology and Mechatronics Engineering Conference (ITOEC), Chongqing, China, 14–16 December 2018; pp. 1412–1416.
44. Li, D.; Chen, M.; Gao, C.; He, S.; Zhang, H. Research on the New Index System of Load Characteristic Based on Demand Response. In Proceedings of the IEEE 7th Annual International Conference on CYBER Technology in Automation, Control, and Intelligent Systems (CYBER), Honolulu, HI, USA, 31 July–4 August 2017; pp. 933–937.
45. Commission Regulation (EU) 2016/631 of 14 April 2016 Establishing a Network Code on Requirements for Grid Connection of Generators (Text with EEA Relevance). *Off. J. Eur. Union* **2016**, *112*, 67.